Journal of Photochemistry and Photobiology A: Chemistry 199 (2008) 64–72

Contents lists available at ScienceDirect

Journal of Photochemistry and Photobiology A: Chemistry

journal homepage: www.elsevier.com/locate/jphotochem

Cotton textile fibres coated by Au/TiO_2 films: Synthesis, characterization and self cleaning properties

M.J. Uddin, F. Cesano, D. Scarano, F. Bonino, G. Agostini, G. Spoto, S. Bordiga, A. Zecchina*

Nanostructured Interfaces and Surfaces (NIS), Centre of Excellence, Department of Chemistry IFM, University of Turin, Via P. Giuria 7, I-10125 Torino, Italy

ARTICLE INFO

Article history:
Received 11 December 2007
Received in revised form 24 April 2008
Accepted 5 May 2008
Available online 15 May 2008

Keywords:
Self cleaning textile
Smart textile
Photocatalysis
Titania
Au/TiO_2
Ag/TiO_2 and methylene blue (MB) photodegradation

ABSTRACT

Au/TiO_2 cotton nanocomposite textile was prepared at low temperature (~100 °C) by sol–gel and photodeposition process designed for practical applications. The Au/TiO_2 nanoparticles have been found to form a homogeneous thin film on the fibre surface and to show efficient photocatalytic properties upon exposure to solar light. Stains cleaning measurements showed that the gold/TiO_2-coated cotton fibres possess photocatalytic activity higher than that of TiO_2-cotton fibres. For this reason the produced composite cotton fibres display high potential and commercial importance for visible light self cleaning properties. The original and treated fibres have been characterized by several techniques (SEM, HRTEM, FTIR, Raman, UV–vis spectroscopy and XRD).

1. Introduction

Because of its excellent photocatalytic properties, high surface area TiO_2 in form of thin films opens a wide scenario of practical applications in environmental purification [1,2]. Photocatalytic degradation on TiO_2 of many substances (4-chloro-2-methylphenol [3], gaseous alcohols [4], isothiazolin-3-ones [5], formaldehyde [6], 3-amino-2-chloropyridine [7], acid orange [8], phenol [9], 4-chlorophenol, 2,5-dichlorophenol, 2,4,5-trichlorophenol, 1,3,5-trihydroxybenzene, 2,3-dihydroxynaphthalene [10], methylene blue in solution phase [11] and diuron on flexible industrial photoresistant paper [12]) has been studied under various illumination conditions and confirmed the excellent properties of this material. This has encouraged the research of new synthetic method that allows its use directly in manufacturing of smart self cleaning textiles. Among these research lines, the synthesis of: (a) anatase nanocrystals deposited on cotton fabrics from titanium isopropoxide (TIP) solutions at $T \leq 100$ °C by sol–gel process with hydrothermal treatment [13] and more recently (b) bleached and mercerized cotton textile fibres activated by RF or MW-plasma and UV-irradiation can be recalled. As far as procedure (b) is concerned, the objective was to introduce negatively charged functional groups which are known to interact with the TiO_2 powder and TiO_2 colloids to anchor TiO_2 on cotton textile [14,15]. In our previous works [16,17] we have described a simple and repeatable anchoring procedure of the TiO_2 and Ag/TiO_2 nanophase to the cellulose fibres by means of sol–gel technique to produce self cleaning, antibacterial and photochromic textiles.

The aim of our current study is to improve the self cleaning properties by developing a simple and repeatable anchoring procedure of a Au/TiO_2 nanophase on cotton fibres. This strategy is justified by the known fact that a significant increase in photocatalytic decomposition of oxalic acid, as compared to unmodified titania, was observed for Au-modified samples [18,19]. A maximum in the photocatalytic activity with the Au-modified samples has been registered in case of 0.16 wt.% Au. At this content the activity of the Au-modified TiO_2 is approximately double that of the unmodified support [18,19]. The structure of the anchored phase was determined by accurate characterizations with several physical methods (XRD, SEM, TEM, UV–vis, IR etc.) The photodegradation of MB and the photostability of the Au/TiO_2 film on the cotton fibre upon prolonged exposure to light have been determined under visible light irradiation and compared with that of the fibre covered with Ag/TiO_2. To check the reuse of the Au/TiO_2-covered fibres, multiple adsorption–photodegradation cycles have been performed. Then it is shown that, due to gold nanoparticles incorporated in the nanoporous titania film, cotton textile with more efficient self

* Corresponding author. Tel.: +39 011 6707860; fax: +39 011 6707855.
E-mail address: adriano.zecchina@unito.it (A. Zecchina).

1010-6030/$ – see front matter © 2008 Elsevier B.V. All rights reserved.
doi:10.1016/j.jphotochem.2008.05.004

cleaning activity and purple colour can be developed. It must be underlined that our adopted method is different from the other ones [14,15,20], because an organic amine was used in the sol to stabilize the solution for long time. This method should be very suitable for industrial applications without using special equipment. In this study, we have prepared Au dispersed TiO_2 thin films using the liquid phase deposition (LPD) method by adding a tetrachloroauric acid ($HAuC1_4$) aqueous solution.

2. Experimental

2.1. Materials

Pure cotton fibre, 10–15 μm in diameter, from PVS srl (Milano, Italy) were used for the entire process. All chemicals used in this work were procured from Aldrich, Germany and have been used as received. Water used in our experiments was triple distilled and produced in our laboratory.

2.2. Synthesis of Au/TiO_2 thin film

At first the impurities (fat, wax, etc.) of the fibres have been removed by soxlet extraction with acetone for 30 min. Then the fibres have been dried at room temperature for 2 h. An alcoholic (isopropanol) solution of titanium isopropoxide was mixed with a second solution, prepared by mixing dilute HCl (a few drops) and $(CH_3)_2CHOH$, following the procedure described in reference [16]. The so obtained transparent sol was homogenized by magnetic stirring (200 rpm) at atmospheric condition. The formed TiO_2 particles remained in the liquid phase without any opacity for long time (1 week) and could be used to impregnate cotton fibre. After impregnation the extracted samples were placed in a preheated oven at 70 °C to remove the solvent from the fibre and then cured at 95 °C for 5 min to complete the formation of TiO_2 from the precursor. Finally, the impregnated cotton fibre samples were treated in boiling water for 3 h (post curing). The unattached TiO_2 particles were removed from the fibre surface during the post curing. The resultant samples were dried in a preheated oven at 40 °C. The thin film covered cotton fibre is then soaked in 0.001 M $HAuCl_4$ aqueous solution for 1 min. The sample was then dried at room temperature. To obtain gold nanoparticles the sample with $HAuCl_4$–TiO_2 film was irradiated at 308 K (50 mW/cm^2, approx 295–3000 nm, Polymer GN 400 ZS, Helios Italquartz, Italy) for 30 min in air at atmospheric humidity.

2.3. Photocatalytic experiments

Photocatalytic degradation of adsorbed methylene blue (MB) on Au/TiO_2 film covered cotton fibre has been investigated. The simulating solar light irradiation was carried out at 308 K by using a SOL2/500S lamp (honle UV technology, Munchen, Germany) for photocatalytic reactions. The SOL-bulb and the H_2 filter together yield a spectrum, which is very similar to the natural sunlight, ranging from ultraviolet to infrared radiation (approx 295–3000 nm). For this purpose, an aqueous solutions (0.05%, w/v) of reagent grade MB were prepared for impregnation of the pure and of Au/TiO_2-covered cotton fibres. The same quantity of each sample was immersed under mild stirring in the same amount of the solution and remained overnight to complete the adsorption. The samples were then removed from MB solution and were dried at room temperature. From the decreased concentration value of MB in solution, the amount of MB on the fibre was estimated to be 4.0 mg/g of cotton fibre. The samples containing adsorbed MB were then exposed to reproducible solar-like light (50 mW/cm^2) to test their photoactivity. The MB photodecomposition reaction was monitored with a UV–vis spectrometer in the reflectance mode by investigating the evolution of the absorbance upon light exposure. The adsorption and the photocatalytic degradation cycles were repeated three times on the same sample to check the photostability of the Au/TiO_2 film.

2.4. Characterization of Au/TiO_2 film

The morphology of pure and Au/TiO_2 deposited cotton fibres have been investigated by scanning electron microscopy on a SEM instrument (Leica, Stereoscan 420) equipped with energy dispersive spectroscopic (EDS) microanalysis system (OXFORD). Bulk EDS analysis was also performed to verify the elemental composition of the deposited materials on the fibre surface. The Au and TiO_2 particle sizes were determined by high resolution transmission electron microscopy (HRTEM) (JEOL 2000EX instrument, 200 keV).

The UV–vis reflectance spectra have been carried out at room temperature on a PerkinElmer UV-Vis-NIR spectrometer to investigate UV absorption intensities, location of absorption edges and the quantum size effects (if any) of the photocatalyst. The UV–vis spectra have been obtained in the reflectance mode on the dried samples. This procedure is aimed to avoid systematic errors in evaluating the intensities of the specific UV–vis bands of the absorbates because, as it is known, the different fillings of intracrystalline voids by the solvent molecules have an important effect on the scattering properties of the samples [21].

XRD patterns have been collected by means of a Philips PW1830 X-ray diffractometer in a Bragg Brentano configuration to identify the crystal phase and structure. Ni-filtered CoKα radiation, 40 kV with a 20-mA current, has been used. The observed patterns have been analyzed using Philips X'Pert High Score software and compared with standard patterns of International Center of Diffraction Data (ICDD) and Powder Diffraction File (PDF) data bases.

To analyze the cellulose polymer chain quality, before and after the treatment and after a long time exposure to solar-like light, FTIR analysis was performed on the samples by mixing with KBr. The spectra were recorded with a IFS28 spectrometer equipped with a MCT cryodetector at a resolution of 2 cm^{-1}.

Raman spectra have been recorded with a Renishaw in Via Raman Microscope spectrometer equipped with Ar^+ laser beam emitting at 514 nm, at 8.2 mW output power. The photons scattered by the sample were dispersed by a 1800 lines/mm grating monochromator and simultaneously collected on a CCD camera; the collection optic was set at 50× objective.

3. Result and discussion

3.1. SEM, EDS and HRTEM analysis of TiO_2 coatings

The morphology of the obtained samples at the micrometer level is shown in Fig. 1a–d, where the comparison between the SEM images of the treated and virgin cotton fibres are illustrated. From Fig. 1b the presence of natural folds running parallel to the elongation direction of the pure cotton fibre, is imaged. Otherwise, Fig. 1c and d clearly show that the treated fibres are covered by a continuous and homogeneous Au/TiO_2 thin film, which obscures the surface folds below. In addition, the presence of rare gold nanoparticles deposited on the TiO_2 film is evidenced at this degree of resolution (Fig. 1d). The gold nanospheres are indicated by white arrows in the SEM images. The EDS analysis (*figure not shown for the sake of brevity*) of the white spots (Fig. 1d and 2c and d) indicates that the nanospheres are indeed constituted by gold. Fig. 2a illustrates the high resolution SEM image of a portion of TiO_2-covered cotton fibre and shows clearly that the film is homogeneous and continuous. The continuous nature of the Au/TiO_2 films suggests

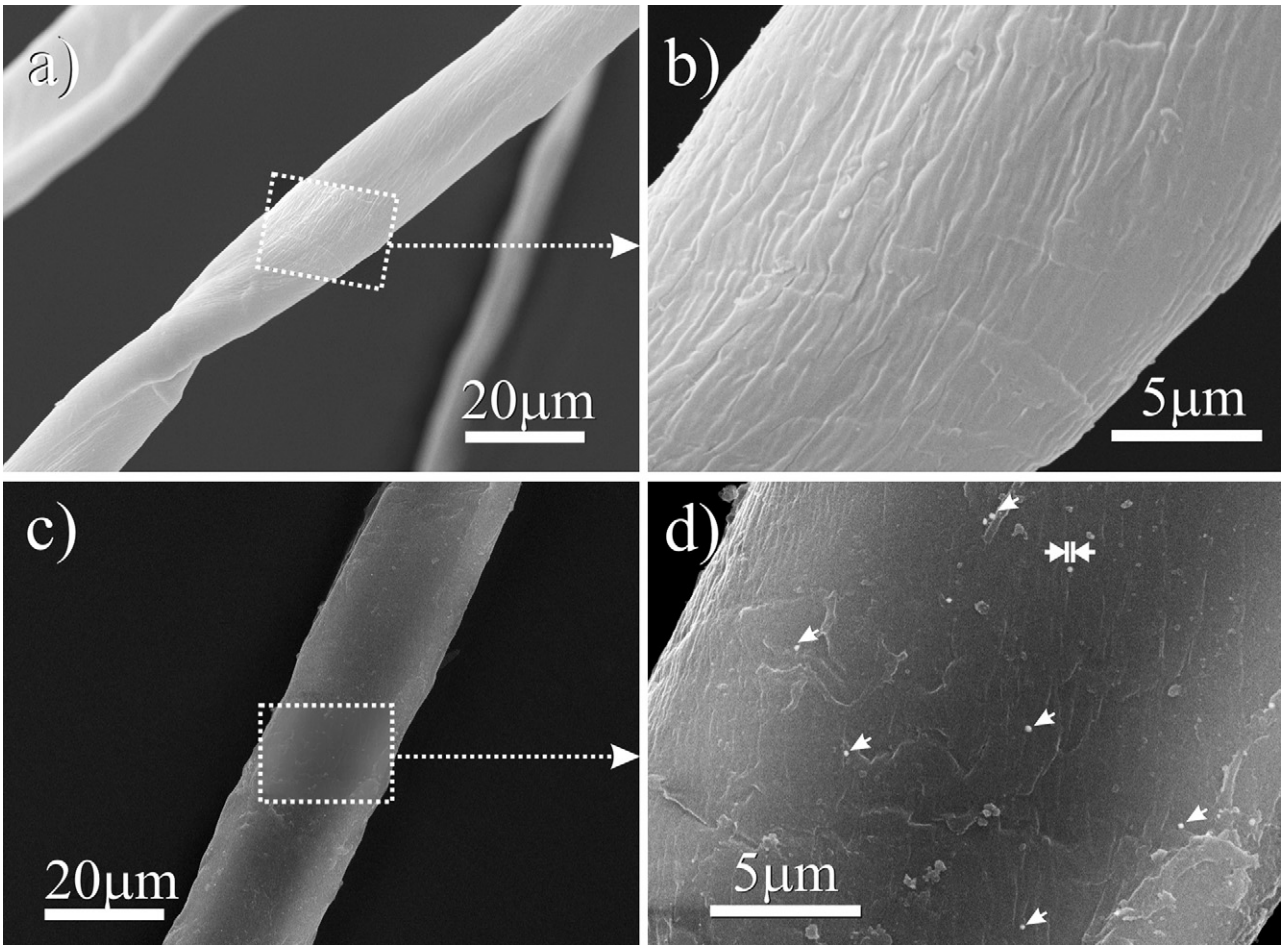

Fig. 1. SEM images of: (a, b) pure cotton fibre and (c, d) Au/TiO_2-covered cotton fibre. Comparison of these images indicates that the regular folds characteristic of the pure fibres are covered by the thin Au/TiO_2 film. The particles, evidenced by arrows in (d), correspond to rare particles (Au) with ~50–150 nm size. The vast majority of the gold particles are not evidenced by SEM.

that pollutant molecules impinging the fibre–Au/TiO_2 composite are interacting preferentially with the photoactive TiO_2 phase covering the fibres (*vide infra*). Fig. 2b–d illustrates the Au/TiO_2 film morphology developed on the cotton surface after burning the Au/TiO_2-covered cotton fibre at 500 °C for 5 h. During this process the cellulose support is removed completely before reaching the temperature of 400 °C [16,17] so allowing the direct observation of the pure TiO_2 envelop. The thickness of the Au/TiO_2 film with cylindrical hollow shape is clearly evidenced in Fig. 2b–d and is about 500 nm. The film thickness, however, is sufficient to cover the natural folds of the fibres present on the surface. Notice that while Fig. 2c represents the secondary backscattered electron image of the above mentioned Au/TiO_2 film, Fig. 2d represents secondary electron image. From the comparison, it is concluded that only the TiO_2 film is well evidenced in Fig. 2d (because the gold particles are obscured) while, on the contrary, Au particles are well evidenced in the Fig. 2c (because the TiO_2 film is obscured). The EDS analysis of Au/TiO_2-covered cotton fibres and of the pure Au/TiO_2 film, after burning the cellulose fibres at 500 °C, are compared in Fig. 3a and b. From the secondary backscattered electron image (Fig. 2c) and the EDS analysis (Fig. 3b), it is confirmed that the white spot shown in the SEM images are indeed gold particles.

In order to investigate the structure of Au and TiO_2 particles forming the film, a portion of the material was collected by scratching the surface and was analyzed by HRTEM. TEM images, reported in Fig. 4, show that the deposited titania film consists of TiO_2 particles almost uniform in size (5–7 nm) (Fig. 4b). The presence of very small particles makes our TiO_2 surfaces different from the surfaces obtained by TiO_2 deposition on glass [22], etc. Our previous HRTEM study of TiO_2 thin film deposited on cotton textile, has indicated that the particle size of the deposited titania on the fibre surface are uniform through the entire surface and the film is uniform and homogeneous [16]. The gold particles are well evidenced in Fig. 4a and b and their size distribution (Fig. 5) (as obtained by using the particles size computing software) indicates that the vast majority is in the 10–12 nm range, whereas only a minor fraction of particles has larger dimensions. The small size of gold and TiO_2 nanoparticles suggests that the exposed surface area of Au/TiO_2 film is very large. This fact together with the above mentioned continuous and homogeneous structure of the film is at the origin of the preferential adsorption of the pollutant on the external layers.

3.2. UV–vis reflectance spectra of Au/TiO_2-covered fibres

Fig. 6 shows the reflectance spectra of pure cotton fibres (curve 1), of anatase TiO_2 (curve 2), of TiO_2-covered fibres (curve 3) and of Au/TiO_2-covered fibres (curve 4). An absorption edge at 29,000 cm^{-1} (curve 3–4), which is slightly upward shifted with respect to that of pure anatase TiO_2 (curve 2), is indicative of the presence of the anatase phase TiO_2. Of course this absorption edge is absent in the curve 1, corresponding to the pure cotton fibres.

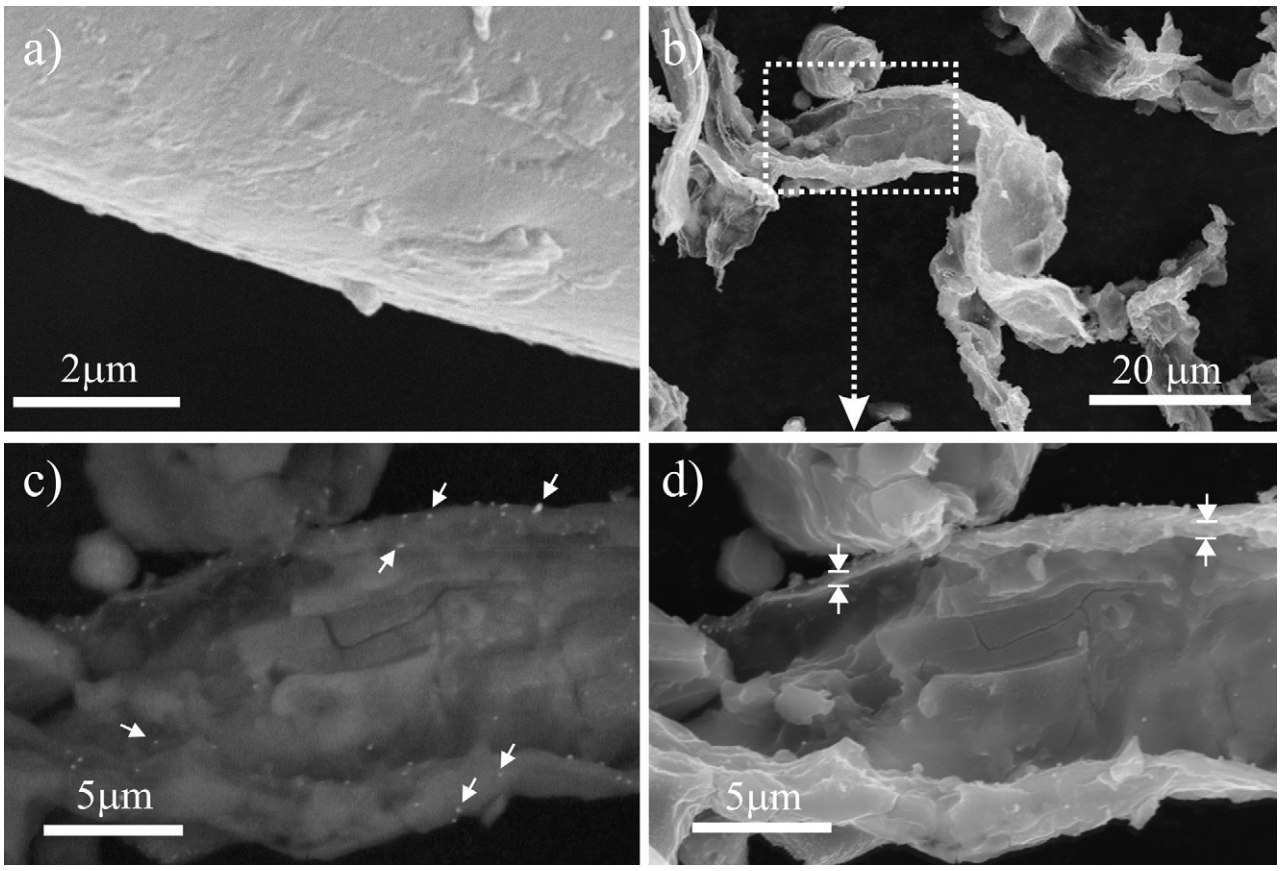

Fig. 2. SEM image of: (a) a TiO_2 film coated cotton fibre (which illustrates the morphology of the TiO_2 film throughout the fibre surface); (b) Au/TiO_2 film collected after combustion at 500 °C for 5 h; (c) back scattered secondary electron image (clearly showing the gold nanoparticles); and (d) secondary electron image (more clearly showing the TiO_2 film thickness). (c and d) refer to the inset reported in (b).

The observed blue shift of the absorption edge on the TiO_2-covered fibres with respect to pure anatase TiO_2 is due to quantum size effects typical of small particles, which have a higher band gap with respect to that of infinite crystals. This observation is in agreement with the results obtained from XRD pattern (*vide infra*) and it is qualitatively confirming SEM and HRTEM results. Furthermore, gold nanoparticles incorporation in the synthesis batch do not modify the size of the TiO_2 crystals, as suggested by TEM images. It is useful to recall that these very small TiO_2 nanoparticles are strongly bounded to the fibres as shown from their good stability toward washing [16,17]. This suggests that the anchoring process of the TiO_2 particles involves the formation of chemical bonds via esterification of the surface OH groups of the fibres with titanols. Coming now to curve 4, the presence of a broad plasmonic absorption centered at ~18,000 cm^{-1}, is associated with the presence of Au particles on the TiO_2 film (since Au^+ does not have any absorption band in this range). The peak position (and hence the purple colour) depends on the particle size [23], which can be estimated to be in the 5–15 nm range. This result is in strong agreement with the TEM images.

3.3. X-ray diffraction (XRD) analysis

The XRD patterns of the pure, TiO_2 and of Au–TiO_2-coated cotton fibres are illustrated in Fig. 7. In the inset, an exploded view shows the patterns of the TiO_2 and Au–TiO_2 impregnated samples together with the anatase peaks position taken from the reference. The intense peak at $2\theta = 26.4°$ is due to the cotton phase. The three broader peaks at $2\theta = 29.44°$, 44.192° and 56.40° are indicative of anatase phase. The remarkable width of these peaks are a direct indication that the particles sizes of the deposited photocatalyst are quite small. From the full width at half maximum (FWHM) of the peaks, by using the Scherrer's equation $L_c = K\lambda/(\beta\cos\theta)$ [24] (where λ is the X-ray wavelength, β is the FWHM of the diffraction line, θ is the diffraction angle, and K is a constant, which has been assumed to be 0.9), an average diameter of the TiO_2 particles is estimated about 5.0 nm. An additional peak at $2\theta = 44.5°$ obtained on the pattern of the Au/TiO_2-covered cotton fibre is corresponding to Au^0 particles on the TiO_2 film. From the width of the $2\theta = 44.5°$ peak, the size of the Au particles is estimated to be ~40 nm. This figure is different from the average particle size estimated in TEM analysis. We believe that this signal is due to the few large particles imaged with TEM and SEM analyses. In fact due to their large size, these particles are expected to give a substantial contribution to the XRD pattern.

3.4. FTIR and Raman spectra

The IR spectra of the cotton fibres before and after TiO_2 and Au/TiO_2 grafting are compared (Fig. 8 curves 1–3). The aim of the experiment was to ascertain whether IR spectroscopy could be informative on the grafting mechanism (which is expected to involve the esterification of OH groups located on the external surface of the fibres) and on any degradation of the cotton fibres caused by the presence of the TiO_2 photoactive phase. The spectrum of the virgin sample (Fig. 8, curve 1) is characterized by an intense and broad band in the 3600–3100 cm^{-1} range, associated with inter- and intra-chain –OH···O groups (τ) of the hydrogen

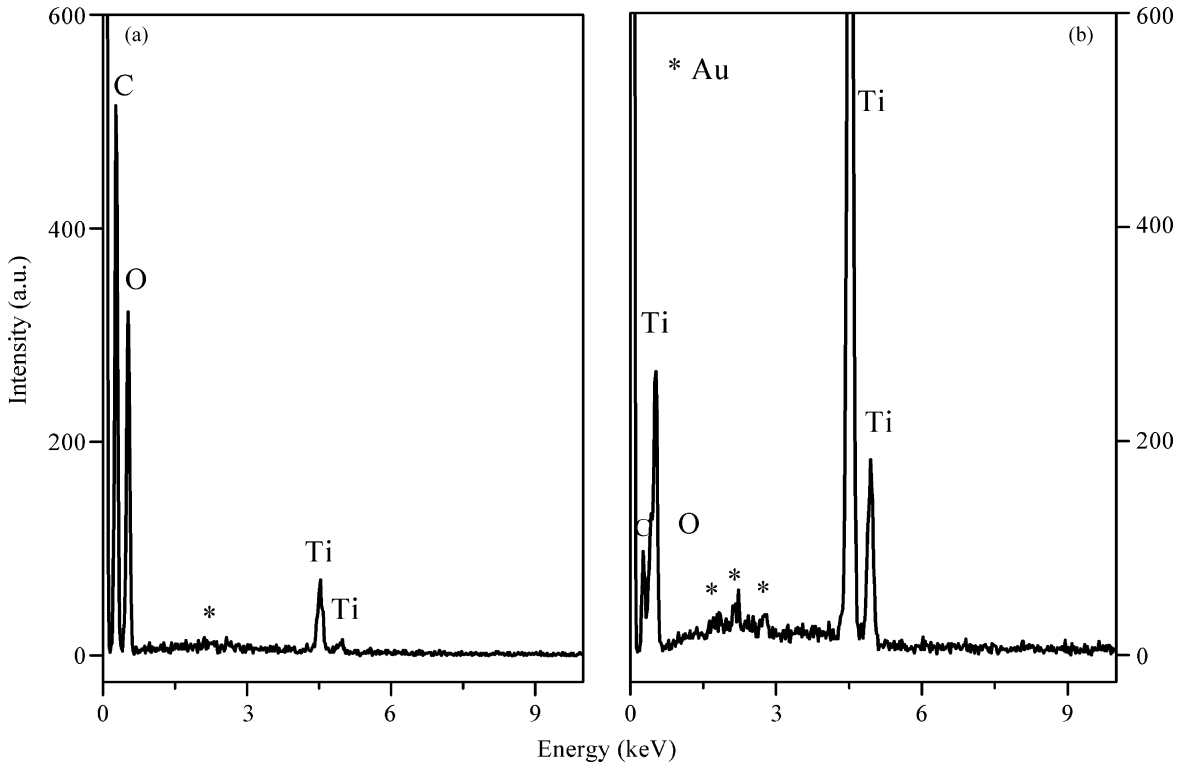

Fig. 3. EDS spectra of: (a) Au/TiO_2-covered cotton fibre; (b) Au/TiO_2 film collected after burning the sample at 500 °C for 5 h in air. In (a) the contribution of the Ti film is highlighted; in (b) the presence of even gold nanoparticles is evidenced. Notice that the residue does not contain the characteristic C and O cellulose components observed on the sample before burning (part a).

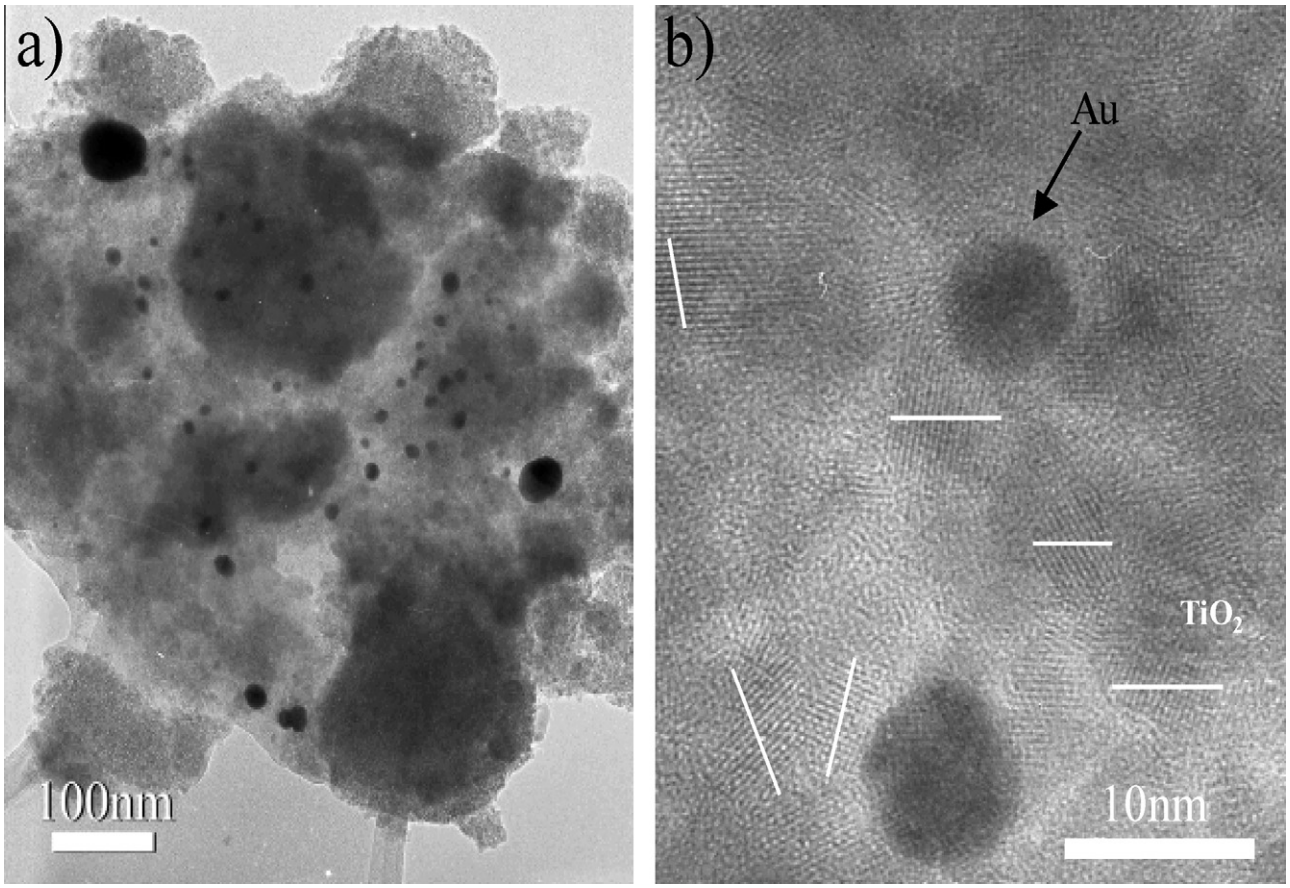

Fig. 4. (a) TEM image of a portion of Au/TiO_2 film; (b) Fourier filtered image of pure anatase particles of a selected area of part a. From these images a mean size of Au nanoparticles of about 10–12 nm along with some larger particle (~40 nm) is highlighted.

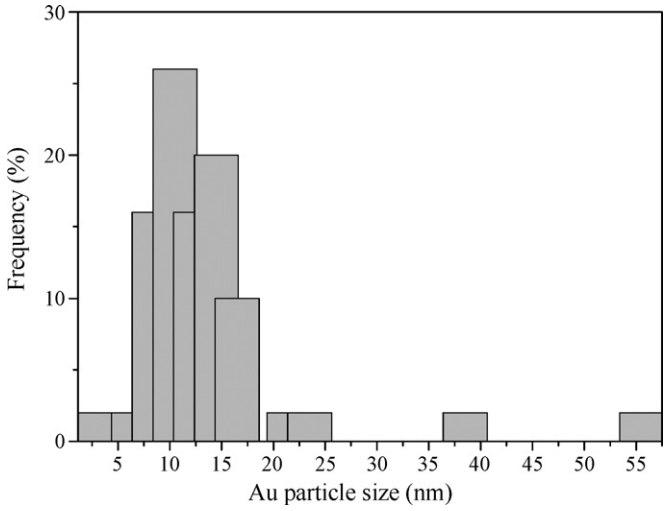

Fig. 5. Au particle size distribution in the TiO_2 film covering the cotton textile, showing that the average particle size is about 10 nm. The rare particles with size in the 40–60 nm range are likely those observed also by SEM (Fig. 2d).

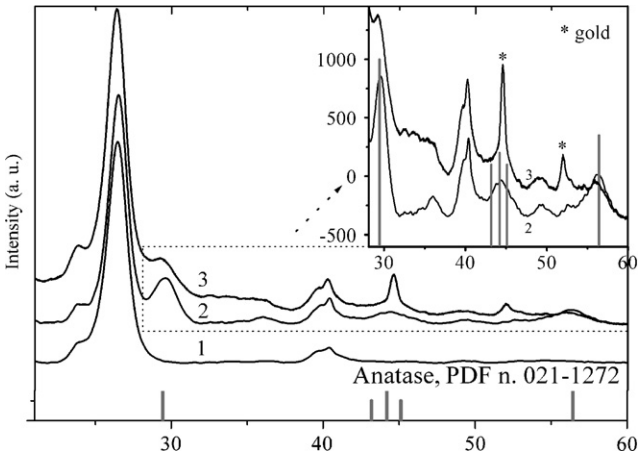

Fig. 7. XRD pattern of: (1) pure cotton; (2) TiO_2-covered cotton and (3) Au/TiO_2-covered cotton fibre. The vertical grey lines and (*) indicate the presence of TiO_2 anatase phase and gold nanoparticles, respectively. The rutile TiO_2 particles are not evidenced in the deposited films.

bonding interacting chains. A peak at ~1600 cm^{-1} is also indicative of the presence of interstitial or adsorbed water. The absorptions in the 3000–2800 and 1450–1350 cm^{-1} ranges are due to the ν(CH) and δ(CH) modes. Finally, the complex absorption in 1250–900 cm^{-1} range is mainly associated with stretching mode of C–O–C groups of the fibre framework. All the above-mentioned groups are mainly located inside the films. Due to the diameter of the fibres (~10 μm) the contribution of the external alcoholic groups, which are expected to actively participate in the anchoring process and hence to be consumed by the grafting procedure, is expected to be small or in the worse case, is negligible. That this is the case is demonstrated by the spectrum of the fibres after grafting (Fig. 8, curve 2 and 3), which is substantially unaltered. It is quite remarkable that being the IR spectrum of the treated sample totally dominated by the spectrum of the fibre, the contribution of the TiO_2 phase (which should appear at $\overline{\nu} < 700\ cm^{-1}$) is also negligible. The photostability of the cellulose fibres is illustrated in Fig. 8, where the curves 4–6 correspond to the sample exposed to solar-like light for 24, 48, 84 h, respectively. It can be seen that the characteristic absorption band at ~3400 cm^{-1} and the complex absorption in the range 1650–1050 cm^{-1} of the fibres are mostly unchanged. These three curves indicate that the chemical structure of cotton fibre is not substantially altered upon exposure to solar-like light. In our opinion, this is due to the homogeneous character of TiO_2 film, which is completely adhering and protecting the fibres from

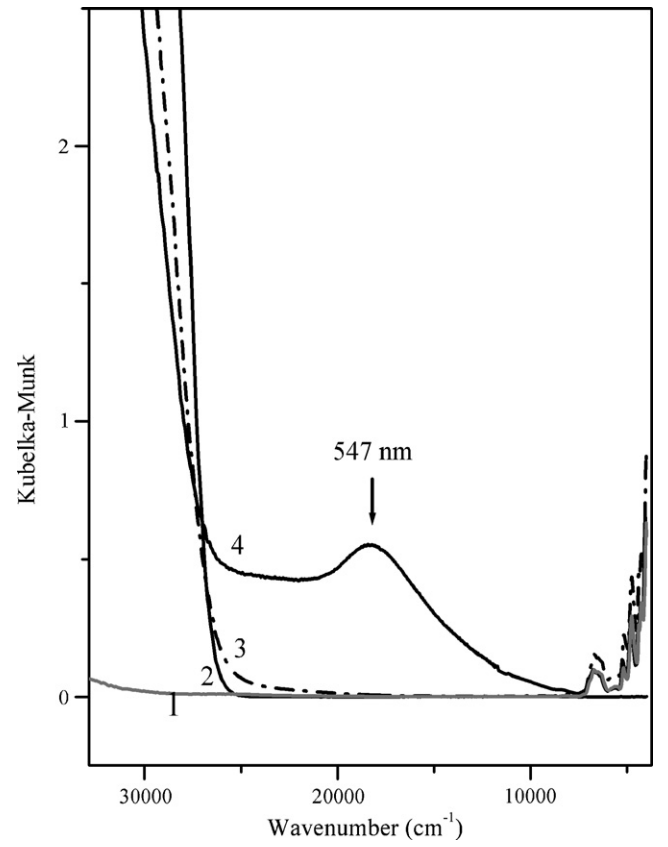

Fig. 6. UV–vis reflectance spectra of: (1) pure cotton fibre; (2) pure anatase TiO_2; (3) TiO_2-covered cotton fibre and (4) Au/TiO_2-covered cotton fibre.

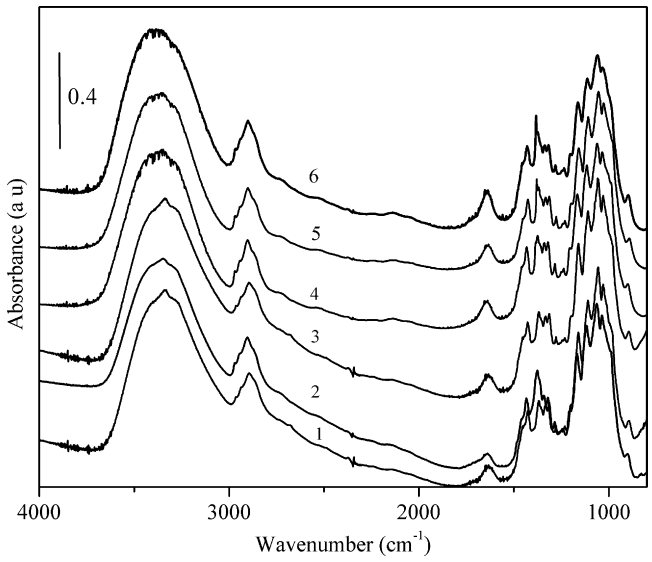

Fig. 8. FTIR spectra of: (1) pure cellulose fibres; (2) TiO_2-covered fibres; (3) Au/TiO_2-covered fibres; (4) cellulose fibre upon 24 h; (5) 48 h and (6) 84 h of solar light exposure. Spectra 3–6 show fibre stability upon sol–gel treatment and solar-like light exposure.

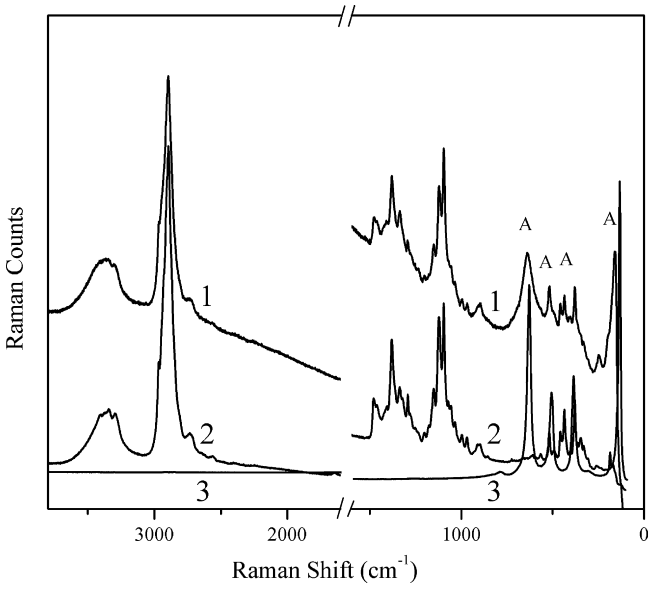

Fig. 9. Raman spectra of: (1) Au/TiO_2-covered cotton; (2) pure cotton fibre and (3) anatase TiO_2. Label A indicates anatase phase TiO_2 on cotton fibre.

aggression of O_2^- and OH• species generated during the exposure to the light.

Contrary to the IR results, shown in Fig. 8, the presence of anatase particles is well evidentiated by the Raman spectroscopy. Fig. 9 curve 1 represents Raman spectrum of Au–TiO_2-covered cotton fibres, while curve 2 reports Raman spectrum of the pure cotton fibres treated with the blank sol (containing all the components, except for the TiO_2 impregnating precursor). For comparison, the Raman spectra of the cotton fibre (curve 2) and of pure anatase TiO_2 (curve 3) are also reported. It can be immediately seen that the spectrum of the Au–TiO_2-coated cotton fibres (curves 1) is dominated by peaks at 158, 406, 517 and 639 cm^{-1}, certainly associated with a TiO_2 phase. This assignment has been confirmed by comparison with the Raman spectrum of pure anatase (curve 3), which shows similar bands at slightly different frequencies (143, 396, 515, and 637 cm^{-1}). It can be remarked that the Raman peaks of the supported TiO_2 are much broader than those of the pure anatase. An explanation of the frequency shifts and of the increase of the peak half width can be advanced by considering the small size of the supported particles. For instance, Raman studies of nanosized anatase, produced by sol–gel route at low temperatures (i.e. lower than 100 °C), report that the vibrational features of TiO_2 are slightly dependent upon the particles sizes and crystallinity [25]. In particular, smaller and less crystalline particles are characterized by broader Raman peaks. Another interesting observation concerns the position of the lowest Raman band at 158 cm^{-1}, which is distinctly upward shifted with respect to that of pure anatase (143 cm^{-1}). Choi et al. [26] have suggested that the Raman bands shift towards higher frequency values as the particles sizes decrease. In particular, when the particles sizes decrease to the nanometer scale, the lowest Raman band shifts towards higher frequency values due to increasing force constants [27,28]. As a similar shift is observed on our sample, it is confirmed that TiO_2 film is constituted by extremely small particles.

3.5. Photocatalytic self cleaning

The photoactivity of the gold–titanium dioxide-coated cotton textiles has been investigated by exposing the samples containing adsorbed methylene blue to solar-like light.

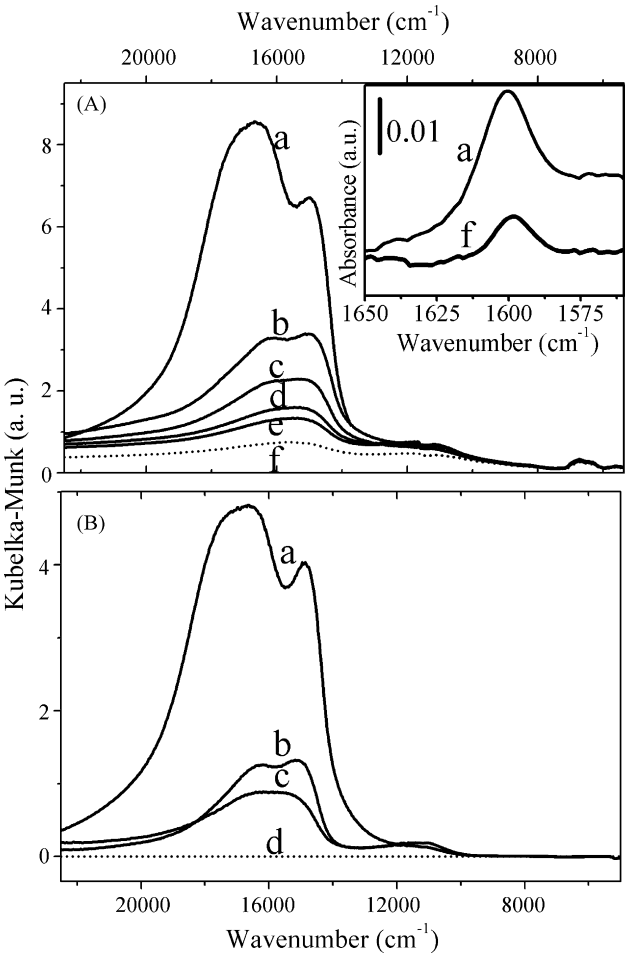

Fig. 10. Spectral changes of methylene blue (MB) spectrum under solar-like light exposure due to photocatalytic degradation. (A) Photodegradation of MB on the TiO_2-covered fibre under artificial solar irradiation: no exposure (curve a), irradiation for 4 h (curve b), 7 h (curve c), 9.5 h (curve d), 11.5 h (curve e) and 19.5 h (curve f). In the inset (curves a and f) FTIR spectra in the 1650–1550 range corresponding to the same curves shown in UV–vis spectra. (B) UV–vis spectral changes of the same stains on Au/TiO_2-covered fibres: no exposure (curve a), 4 h exposure (curve b), 7 h exposure (curve c) and 19.5 h exposure (curve d).

The UV–vis reflectance spectra before (curve a) and after illumination with increasing time obtained on TiO_2-cotton/MB and on Au/TiO_2–cotton/MB systems are compared in Fig. 10A (curves b–f) and Fig. 10B (curves b–d). From this comparison it is inferred that the complex absorption bands in the 20,000–12,000 cm^{-1} interval, due to absorption of MB, change rapidly because TiO_2 promotes the catalytic photodegradation (curves a–f and a–d). This is not unexpected since the photocatalytic activity of TiO_2 is well known [1,29]. Of course the disappearance rate of the band due to adsorbed MB on the TiO_2-covered fibres is much higher than that observed in case of untreated fibres. On the basis of the data reported in the literature [16], the bands at 15,400 and 16,400 cm^{-1} are assigned to the monomeric and aggregated MB (mostly dimeric and trimeric species), respectively, adsorbed on the surface. Under light exposure the aggregate species disappear first, followed by the monomeric ones. Of course the photodegradation effect is lower than that of observed on P25 (Fig. 11).

The photodegradation process can be followed also by the gradual disappearance of the IR bands of adsorbed MB. Among all bands of MB, that at 1600 cm^{-1} can be better monitored, since it falls in a region where the cellulose skeleton is not absorbing. The results are shown in the inset of Fig. 10A. It is worth noticing that

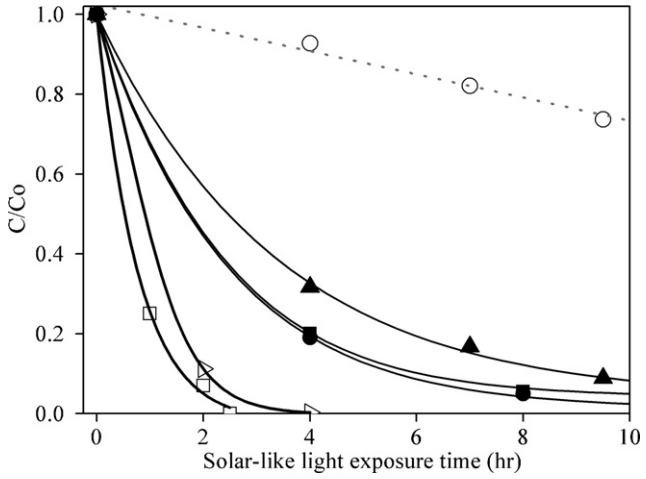

Fig. 11. Photocatalytic MB degradation by Au/TiO_2-covered cellulose fibre upon solar-like light illumination. Photocatalytic degradation of MB on untreated fibres (○), on TiO_2-coated fibres (▲), on Au/TiO_2-coated fibres (■), on Ag/TiO_2-coated fibres (●), on P25 (▷) and on Au/P25 (□).

both UV–vis and IR spectroscopies are unable to clearly reveal the formation of intermediate degradation products during the photocatalytic process. An important result of this investigation is the observation that the TiO_2-covered cotton fibres containing gold particles are more active in MB degradation than those not containing gold (Fig. 11). This is not unexpected. In fact a substantial improvement in photoactivity of gold (0.1–0.8%) dispersed titania [30], specifically containing small gold particles, was observed [31]. In particular, the dispersion of gold nanoparticles on the TiO_2 matrix has a beneficial influence on the organic stains photodegradation [32] and catalysis [19,33]. Two explanations of the beneficial effect of the gold particles are usually advanced. The first explanation is that the gold nanoparticles absorb the light in the visible range and transfer the excitation to TiO_2 photocatalyst, plausibly acting as sensitizer. The second explanation lies on the electron trapping ability of the metal particles which can increase excitation lifetime and stability of generated electrons, so reducing the tendency to recombine hole (h^+) and electron (e^-). On the basis of our experimental data, we cannot make a choice between the two hypothesis.

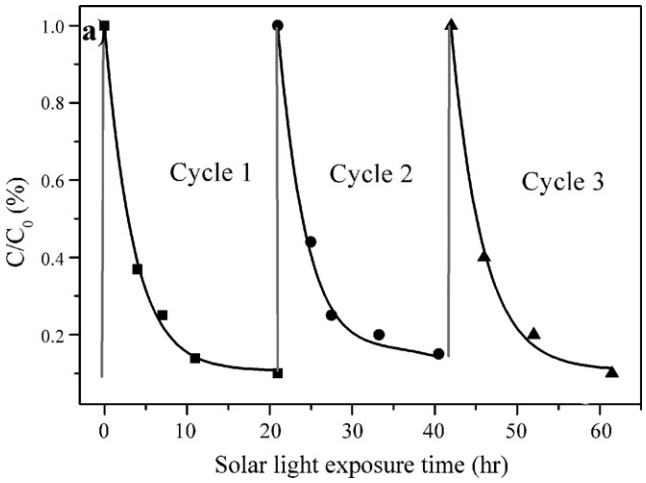

Fig. 12. Photocatalytic activity of Au/TiO_2-covered cotton fibre upon repeated MB adsorption–illumination cycles.

Fig. 12 shows that the photocatalytic efficiency of the Au/TiO_2-coated fibre on degrading MB is unchanged upon repeating cycles. These results suggest that the activity of Au/TiO_2 film is not influenced by successive impregnation steps and this is in agreement with the results shown in our previous study [17].

4. Conclusions

Cotton fibres, covered by a thin Au/TiO_2 film constituted by anatase nanocrystallites strongly adhering to the support, display a purple colour and are photocatalytically active under solar light. The Au/TiO_2-covered cotton fibres show high efficiency in MB photodegradation, so suggesting high photocatalytic self cleaning properties under solar-like light. The sol–gel synthesis method, utilized to cover the cotton fibres with TiO_2 and Au/TiO_2 films, guarantees a great stability towards repeated washing cycles and prolonged photodegradation activity. This stability is promising for possible industrial applications.

Acknowledgements

The authors acknowledge the financial support from Regione Piemonte (Progetto NANOMAT, Docup 2000–2006, Linea 2.4a). M.Jasim Uddin is grateful to AssociazioneTessile e Salute for supporting his PhD fellowship and to Shah Jalal University of Science and Technology, Sylhet-3114, Bangladesh for granting him study leave for the PhD program.

References

[1] A. Fujishima, K. Honda, Nature 238 (1972) 37–38.
[2] A. Fujishima, T.N. Rao, D.A. Tryk, J. Photochem. Photobiol. C-Chem. Rev. 1 (2000) 1–21.
[3] S. Irmak, E. Kusvuran, O. Erbatur, Appl. Catal. B-Environ. 54 (2004) 85–91.
[4] J. Arana, J.M. Dona-Rodriguez, O. Gonzalez-Diaz, E.T. Rendon, J.A.H. Melian, G. Colon, J.A. Navio, J.P. Pena, J. Mol. Catal. A-Chem. 215 (2004) 153–160.
[5] V. Kandavelu, H. Kastien, K.R. Thampi, Appl. Catal. B-Environ. 48 (2004) 101–111.
[6] C.H. Ao, S.C. Lee, J.Z. Yu, J.H. Xu, Appl. Catal. B-Environ. 54 (2004) 41–50.
[7] B.F. Abramovic, V.B. Anderluh, A.S. Topalov, F.F. Gaal, Appl. Catal. B-Environ. 48 (2004) 213–221.
[8] M. Stylidi, D.I. Kondarides, X.E. Verykios, Appl. Catal. B-Environ. 47 (2004) 189–201.
[9] M. Alvaro, C. Aprile, M. Benitez, E. Carbonell, H. Garcia, J. Phys. Chem. B 110 (2006) 6661–6665.
[10] S. Usseglio, P. Calza, A. Damin, C. Minero, S. Bordiga, C. Lamberti, E. Pelizzetti, A. Zecchina, Chem. Mater. 18 (2006) 3412–3424.
[11] A. Houas, H. Lachheb, M. Ksibi, E. Elaloui, C. Guillard, J.M. Herrmann, Appl. Catal. B-Environ. 31 (2001) 145–157.
[12] M. El Madani, C. Guillard, N. Perol, J.M. Chovelon, M. El Azzouzi, A. Zrineh, J.M. Herrmann, Appl. Catal. B 65 (2006) 70–76.
[13] W.A. Daoud, J.H. Xin, J. Am. Ceram. Soc. 87 (2004) 953–955.
[14] T. Yuranova, D. Laub, J. Kiwi, Catal. Today 122 (2007) 109–117.
[15] T. Yuranova, A.G. Rincon, A. Bozzi, S. Parra, C. Pulgarin, P. Albers, J. Kiwi, J. Photochem. Photobiol. A-Chem. 161 (2003) 27–34.
[16] M.J. Uddin, F. Cesano, F. Bonino, S. Bordiga, G. Spoto, D. Scarano, A. Zecchina, J. Photochem. Photobiol. A-Chem. 189 (2007) 286–294.
[17] M.J. Uddin, F. Cesano, F. Bonino, S. Bertarione, S. Bordiga, G. Spoto, D. Scarano, A. Zecchina, J. Photochem. Photobiol. A-Chem 196 (2008) 165–173.
[18] G. Mele, G. Ciccarella, G. Vasapollo, E. Garcia-Lopez, L. Palmisano, M. Schiavello, Appl. Catal. B-Environ. 38 (2002) 309–319.
[19] A. Corma, P. Serna, H. Garcia, J. Am. Chem. Soc. 129 (2007) 6358–6359.
[20] Y.C. Dong, L.W. Zhang, R.H. Liu, T. Zhu, J. Appl. Polym. Sci. 99 (2006) 286–291.
[21] F. Bonino, A. Damin, G. Ricchiardi, M. Ricci, G. Spano, R. D'Aloisio, A. Zecchina, C. Lamberti, C. Prestipino, S. Bordiga, J. Phys. Chem. B 108 (2004) 3573–3583.
[22] W.Y. Gan, K. Chiang, M. Brungs, R. Amal, H. Zhao, Int. J. Nanotechnol. 4 (2007) 574–587.
[23] S. Deki, Y. Aoi, H. Yanagimoto, K. Ishii, K. Akamatsu, M. Mizuhata, A. Kajinami, J. Mater. Chem. 6 (1996) 1879–1882.
[24] L.S. Birks, H. Friedman, J. Appl. Phys. 17 (1946) 687–692.
[25] D. Bersani, G. Antonioli, P.P. Lottici, T. Lopez, J. Non-Cryst. Solids 234 (1998) 175–181.
[26] H.C. Choi, Y.M. Jung, S.B. Kim, Vib. Spectrosc. 37 (2005) 33–38.

[27] J. Rockenberger, L. Troger, A. Kornowski, T. Vossmeyer, A. Eychmuller, J. Feldhaus, H. Weller, J. Phys. Chem. B 101 (1997) 2691–2701.
[28] M.A. Marcus, M.P. Andrews, J. Zegenhagen, A.S. Bommannavar, P. Montano, Phys. Rev. B 42 (1990) 3312–3316.
[29] A. Fujishima, K. Kobayakawa, K. Honda, J. Electrochem. Soc. 122 (1975) 1487–1489.
[30] V. Iliev, D. Tomova, R. Todorovska, D. Oliver, L. Petrov, D. Todorovsky, M. Uzunova-Bujnova, Appl. Catal. A-Gen. 313 (2006) 115–121.
[31] M. Valden, X. Lai, D.W. Goodman, Science 281 (1998) 1647–1650.
[32] L. Armelao, D. Barreca, G. Bottaro, A. Gasparotto, C. Maccato, C. Maragno, E. Tondello, U.L. Stangar, M. Bergant, D. Mahne, Nanotechnology (2007) 18.
[33] A. Corma, P. Serna, Science 313 (2006) 332–334.